

Gold–Gold Interactions as Crystal Engineering Design Elements in Heterobimetallic Coordination Polymers

Daniel B. Leznoff,^{*,†} Bao-Yu Xue,[†] Raymond J. Batchelor,[†] Frederick W. B. Einstein,[†] and Brian O. Patrick[‡]

Departments of Chemistry, Simon Fraser University, 8888 University Drive, Burnaby, BC, V5A 1S6 Canada, and University of British Columbia, 2036 Main Mall, Vancouver, BC, V6T 1Z1 Canada

Received July 16, 2001

A series of coordination polymers containing Cu(II) and $[\text{Au}(\text{CN})_2]^-$ units has been prepared. Most of their structures incorporate attractive gold–gold interactions, thus illustrating that such “aurophilic” interactions can be powerful tools for increasing structural dimensionality in supramolecular systems. $[\text{Cu}(\text{tren})\text{Au}(\text{CN})_2][\text{Au}(\text{CN})_2]$ (**1**, tren = tris(2-ethylamino)amine) forms a cation/anion pair, which is weakly linked by hydrogen bonds but not by aurophilic interactions. $[\text{Cu}(\text{en})_2\text{Au}(\text{CN})_2][\text{Au}(\text{CN})_2]$ (**2-Au**, en = ethylenediamine) is a 2-D system composed of a chain of $[\text{Au}(\text{CN})_2]^-$ anions and another chain of $[(\text{en})_2\text{Cu}-\text{NCAuCN}]^+$ cations; short Au–Au bonds of 3.1405(2) Å connect the anions. This bond is shorter than that observed in the analogous silver(I) structure, **2-Ag**. The average M–C bond lengths of 1.984(8) Å in **2-Au** are significantly shorter than those found in **2-Ag**, suggesting that Au(I) is smaller than Ag(I). $\text{Cu}(\text{dien})[\text{Au}(\text{CN})_2]_2$ (**3**, dien = diethylenetriamine) forms a 1-D chain of tetranuclear $[\text{Au}(\text{CN})_2]^-$ units that are bound to $[\text{Cu}(\text{dien})]$ centers. Aurophilic interactions of ca. 3.35 Å hold the tetramer together. $\text{Cu}(\text{tmeda})[\text{Au}(\text{CN})_2]_2$ (**4**, tmeda = *N,N,N',N'*-tetramethylethylenediamine) forms a 3-D network by virtue of aurophilic interactions of 3.3450(10) and 3.5378(8) Å. Altering the Cu:Au stoichiometry yields $\text{Cu}(\text{tmeda})[\text{Au}(\text{CN})_2]_{1.5}(\text{ClO}_4)_{0.5}$ (**5**), which has an unusual 2-D rhombohedral layer structure (space group *R32*). Complex **5** is composed of three mutually interpenetrating $\text{Cu}[\text{Au}(\text{CN})_2]_{1.5}$ networks which are interconnected by aurophilic interactions of 3.4018(7) and 3.5949(8) Å. Weak antiferromagnetic coupling is observed in **2** and **5**.

Introduction

The design and synthesis of self-assembling supramolecular systems is an area of intense interest as a route to the rational generation of functional materials.^{1,2} Of the available implements in the crystal engineering “toolbox” used to create such materials, hydrogen-bonding interactions are perhaps the most widely applied, both to generate systems with a particular desired supramolecular topology and also to increase structural dimensionality in general.³ This increase is important as high-dimensionality systems often show useful magnetic,⁴ nonlinear optical,⁵ conducting,⁶ or zeolitic^{7,8} properties. In inorganic coordination polymers, the choice of metal/ligand combination

helps control both the supramolecular topology and the dimensionality,^{9,10} but the incorporation of hydrogen-bonding moieties into such systems can also greatly influence the crystal structure and its dimensionality.¹¹

Gold(I) centers are known to form attractive gold–gold interactions with themselves which have order-of-magnitude strengths comparable to hydrogen bonds^{12–14} and thus, in principle, could also be used to control supramolecular structure and dimensionality. Although many homometallic Au(I) polymers formed by virtue of these “aurophilic” interactions have

* Corresponding author. Tel: 1-604-291-4887. Fax: 1-604-291-3765. E-mail: dleznoff@sfu.ca.

[†] Simon Fraser University.

[‡] University of British Columbia.

- (1) *Crystal Engineering: From Molecules and Crystals to Materials*; Braga, D., Grepioni, F., Orpen, A. G., Eds.; Kluwer Academic Publishers: Dordrecht, 1999.
- (2) Ouahab, L. *Chem. Mater.* **1997**, *9*, 1909 and references therein.
- (3) (a) Desiraju, G. R. *Crystal Engineering. The Design of Organic Solids*; Elsevier: Amsterdam, 1989. (b) Braga, D.; Grepioni, F.; Desiraju, G. R. *Chem. Rev.* **1998**, *98*, 1375. (c) Cantrill, S. J.; Pease, A. R.; Stoddart, J. F. *J. Chem. Soc., Dalton Trans.* **2000**, 3715 and references therein. (d) Aakeroy, C. B.; Seddon, K. R. *Chem. Soc. Rev.* **1993**, *22*, 397.
- (4) (a) Miller, J. S. *Inorg. Chem.* **2000**, *39*, 4392. (b) *Magnetism: A Supramolecular Function*; Kahn, O., Ed.; Kluwer Academic Publishers: Dordrecht, 1996.
- (5) (a) *Optoelectronic Properties of Inorganic Compounds*; Roundhill, D. M., Fackler, J. P., Jr., Eds.; Plenum Press: New York, 1999. (b) Marks, T. J.; Ratner, M. A. *Angew. Chem., Int. Ed. Engl.* **1995**, *34*, 155. (c) Dalton, L. R.; Harper, A. W.; Ghosn, R.; Steier, W. H.; Ziari, M.; Fetterman, H.; Shi, Y.; Mustacich, R. V.; Jen, A. K.-Y.; Shea, K. J. *Chem. Mater.* **1995**, *7*, 1060.

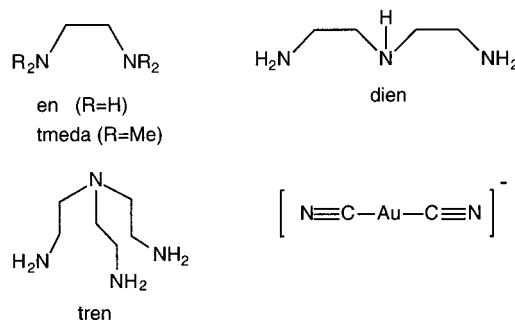
- (6) (a) *Handbook of Conducting Polymers*, 2nd ed.; Skotheim, T. A., Elsenbaumer, R. L., Reynolds, J. R., Eds.; M. Dekker: New York, 1998. (b) *NATO ARW Supramolecular Engineering of Synthetic Metallic Materials: Conductors and Magnets*; Veciana, J., Rovira, C., Amabilino, D., Eds.; Springer: Berlin, 1998; Vol. C518.
- (7) (a) Yaghi, O. M.; Li, H.; Davis, C.; Richardson, D.; Groy, T. L. *Acc. Chem. Res.* **1998**, *31*, 474. (b) Hagrman, P. J.; Hagrman, D.; Zubieta, J. *Angew. Chem., Int. Ed.* **1999**, *38*, 2638.
- (8) Iwamoto, T. In *Inclusion Compounds*; Atwood, J. L., Davies, J. E. D., MacNicol, D. D., Eds.; Oxford University Press: London, U.K., 1991; Vol. 5, p 177.
- (9) Blake, A. J.; Champness, N. R.; Hubberstey, P.; Li, W.-S.; Withersby, M. A.; Schröder, M. *Coord. Chem. Rev.* **1999**, *183*, 117.
- (10) *Comprehensive Supramolecular Chemistry. Volume 7. Solid State Supramolecular Chemistry: Two and Three-dimensional Inorganic Networks*; Lehn, J. M., Atwood, J. L., Davies, J. E. D., MacNicol, D. D., Vögtle, F., Alberti, G., Bein, T., Eds.; Pergamon Press: Oxford, 1996.
- (11) (a) Zaworotko, M. J. *Chem. Soc. Rev.* **1994**, *23*, 283. (b) Subramanian, S.; Zaworotko, M. J. *Coord. Chem. Rev.* **1994**, *137*, 357. (c) Bernhardt, P. V. *Inorg. Chem.* **1999**, *38*, 3481.
- (12) Schmidbaur, H. *Chem. Soc. Rev.* **1995**, 391.
- (13) Pyykkö, P. *Chem. Rev.* **1999**, *97*, 5597.
- (14) (a) Tzeng, B.-C.; Schier, A.; Schmidbaur, H. *Inorg. Chem.* **1999**, *38*, 3978. (b) Hollatz, C.; Schier, A.; Schmidbaur, H. *J. Am. Chem. Soc.* **1997**, *119*, 8115.

been studied,¹⁵ heterometallic polymers incorporating such gold–gold interactions are uncommon.

The linear building block dicyanoaurate, $[\text{Au}(\text{CN})_2]^-$,¹⁶ is a convenient unit with which to explore the use of aurophilicity as a supramolecular design element. It can form polymers in a fashion similar to other metal–cyanide anions, but is unique in that its central Au(I) atom is prone to forming gold–gold bonds both in solution¹⁷ and in the solid state.^{18–20} Other metal–cyanide anions have played a prominent role in the design of supramolecular coordination polymers^{21–23} as they readily form strong bonds with transition metal cations and are excellent mediators of electronic and magnetic exchange, as demonstrated by their ubiquitous use in the synthesis of Prussian-blue type, high- T_c molecule-based magnets.²⁴ However, although many coordination polymers incorporating octahedral $[\text{M}(\text{CN})_6]^{n-}$ units have been reported,²² there are relatively few coordination polymers that contain the two-coordinate, linear $[\text{Au}(\text{CN})_2]^-$ ^{25–30} or $[\text{Ag}(\text{CN})_2]^-$ ^{31–34} building blocks.

We have been exploring the concept of using aurophilic interactions as a *tool* to create heterometallic supramolecular architectures.^{25,26,35} In an effort to examine the impact of aurophilic interactions in a systematic fashion, we reacted a

Scheme 1. Ligands Used in This Work



series of copper(II)–amine complexes with $\text{K}[\text{Au}(\text{CN})_2]$, controlling, with the capping amine ligands, the number of copper(II) coordination sites available to bind cyanide–nitrogen donors. A series of compounds ranging from discrete ionic systems to 3-D arrays were produced, in which aurophilic interactions play a prominent role in determining the solid-state structures, thus illustrating their ability to vary and increase structural dimensionality.

Experimental Section

General Procedures and Physical Measurements. Unless otherwise stated all manipulations were performed in air using purified solvents. The amine ligands en, tmeda, dien and tren and all other reagents were obtained from commercial sources and used as received. (Ligand abbreviations: tren = tris(2-ethylamino)amine; cyclen = 1,4,7,10-tetraazacyclododecane; dien = diethylenetriamine; en = ethylenediamine; tmeda = N,N,N',N' -tetramethylethylenediamine.) IR spectra were obtained using a Bomem Michelson 120 FTIR spectrometer. Thermogravimetric analysis data were collected using a Shimadzu TGA-50 instrument in an air atmosphere. Microanalyses (C, H, N) were performed at Simon Fraser University by Mr. Miki Yang.

Variable temperature magnetic susceptibility data were collected using a Quantum Design SQUID MSMS-5S magnetometer working down to 2 K at 1 T field strength. Samples were placed in a gelatin capsule and suspended in a clear plastic straw. The data were corrected for TIP, the diamagnetism of the sample holder, and the constituent atoms (by use of Pascal constants).³⁶

Synthetic Procedures. CAUTION: Although we have experienced no difficulties, perchlorate salts are potentially explosive and thus should only be prepared in small quantities and handled with care.

$[\text{Cu}(\text{tren})\text{Au}(\text{CN})_2][\text{Au}(\text{CN})_2]$ (1). To a 10 mL aqueous solution of $\text{Cu}(\text{ClO}_4)_2 \cdot 6\text{H}_2\text{O}$ (0.037 g, 0.1 mmol) was added a 2 mL aqueous solution of tren (stock solution, 0.1 mmol). A 2 mL aqueous solution of $\text{KAu}(\text{CN})_2$ (0.059 g, 0.2 mmol) was added dropwise with stirring to this blue solution, which was filtered and cooled overnight to yield $[\text{Cu}(\text{tren})\text{Au}(\text{CN})_2][\text{Au}(\text{CN})_2]$ (1) as small blue crystals. Yield: 0.055 g (78%). Anal. Calcd for $\text{C}_{10}\text{H}_{18}\text{N}_8\text{Au}_2\text{Cu}$: C, 16.97; H, 2.56; N, 15.83. Found: C, 16.69; H, 2.54; N, 16.01. IR (KBr): 2205 (ν_{CN}), 2153 (ν_{CN}), 2141 (ν_{CN}), 1578, 1474, 1381, 1256, 1094, 1068, 995, 978, 910, 750, 672, 619 cm^{-1} . Single crystals suitable for X-ray structural analysis were obtained by slow evaporation of an aqueous solution of 1.

$[\text{Cu}(\text{en})_2\text{Au}(\text{CN})_2][\text{Au}(\text{CN})_2]$ (2). The preparation was analogous to that of 1. $[\text{Cu}(\text{en})_2][\text{Au}(\text{CN})_2]_2$ (2) slowly precipitated from the

- (15) (a) Schneider, W.; Angermaier, K.; Sladek, A.; Schmidbauer, H. Z. *Naturforsch.* **1996**, *51B*, 790. (b) Hunks, W. J.; Jennings, M. C.; Puddephatt, R. J. *Inorg. Chem.* **1999**, *38*, 5930. (c) Perreault, D.; Drouin, M.; Michel, A.; Harvey, P. D. *Inorg. Chem.* **1997**, *36*, 5231. (d) Van Calcar, P. M.; Olmstead, M. M.; Balch, A. L. *J. Chem. Soc., Chem. Commun.* **1995**, 1773. (e) Vicente, J.; Chicote, M.-T.; Abrisqueta, M.-D.; Guerrero, R.; Jones, P. G. *Angew. Chem., Int. Ed. Engl.* **1997**, *36*, 1203.
- (16) Rosenzweig, A.; Cramer, D. T. *Acta Crystallogr.* **1959**, *12*, 709.
- (17) Rawashdeh-Omary, M. A.; Omary, M. A.; Patterson, H. H. *J. Am. Chem. Soc.* **2000**, *122*, 10371.
- (18) (a) Blom, N.; Ludi, A.; Bürgi, H.-B.; Ticky, K. *Acta Crystallogr.* **1984**, *C40*, 1767. (b) Fischer, P.; Mesot, J.; Lucas, B.; Ludi, A.; Patterson, H.; Hewat, A. *Inorg. Chem.* **1997**, *36*, 2791.
- (19) Blom, N.; Ludi, A.; Bürgi, H.-B. *Acta Crystallogr.* **1984**, *C40*, 1770.
- (20) Cramer, R. E.; Smith, D. W.; VanDorpe, W. *Inorg. Chem.* **1998**, *37*, 5895.
- (21) Dunbar, K. R.; Heintz, R. A. *Prog. Inorg. Chem.* **1997**, *45*, 283.
- (22) Ohba, M.; Okawa, H. *Coord. Chem. Rev.* **2000**, *198*, 313.
- (23) Vahrenkamp, H.; Geib, A.; Richardson, G. N. *J. Chem. Soc., Dalton Trans.* **1997**, 3643.
- (24) Verdaguer, M.; Bleuzen, A.; Marvaud, V.; Vaissermann, J.; Seuleiman, M.; Desplanches, C.; Scullier, A.; Train, C.; Garde, R.; Gelly, G.; Lomenech, C.; Rosenman, I.; Veillet, P.; Cartier, C.; Villain, F. *Coord. Chem. Rev.* **1999**, *190–192*, 1023.
- (25) Leznoff, D. B.; Xue, B.-Y.; Patrick, B. O.; Sanchez, V.; Thompson, R. C. *Chem. Commun.* **2001**, 259.
- (26) Leznoff, D. B.; Xue, B.-Y.; Stevens, C. L.; Storr, A.; Thompson, R. C.; Patrick, B. O. *Polyhedron* **2001**, *20*, 1247.
- (27) Chu, I. K.; Shek, I. P. Y.; Siu, K. W. M.; Wong, W.-T.; Zuo, J.-L.; Lau, T.-C. *New J. Chem.* **2000**, *24*, 765.
- (28) Yeung, W.-F.; Wong, W.-T.; Zuo, J.-L.; Lau, T.-C. *J. Chem. Soc., Dalton Trans.* **2000**, 629.
- (29) (a) Stier, A.; Range, K.-J. *Z. Naturforsch.* **1996**, *51b*, 698. (b) Stier, A.; Range, K.-J. *Z. Kristallogr.* **1997**, *212*, 51. (c) Assefa, Z.; Shankle, G.; Patterson, H. H.; Reynolds, R. *Inorg. Chem.* **1994**, *33*, 2187. (d) Assefa, Z.; Staples, R. J.; Fackler, J. P., Jr.; Patterson, H. H.; Shankle, G. *Acta Crystallogr.* **1995**, *C51*, 2527.
- (30) (a) Hoskins, B. F.; Robson, R.; Scarlett, N. V. Y. *Angew. Chem., Int. Ed. Engl.* **1995**, *34*, 1203. (b) Abrahams, S. C.; Zyontz, L. E.; Bernstein, J. L. *J. Chem. Phys.* **1982**, *76*, 5458. (c) Abrahams, S. C.; Bernstein, J. L.; Liminga, R.; Eisenmann, E. T. *J. Chem. Phys.* **1980**, *73*, 4585.
- (31) (a) Soma, T.; Yuge, H.; Iwamoto, T. *Angew. Chem., Int. Ed. Engl.* **1994**, *33*, 1665. (b) Soma, T.; Iwamoto, T. *Chem. Lett.* **1994**, 821.
- (32) (a) Cernák, J.; Chomic, J.; Graveriau, P.; Orendáčová, A.; Orendáč, M.; Kováč, J.; Feher, A.; Kappenstein, C. *Inorg. Chim. Acta* **1998**, *281*, 134. (b) Kappenstein, C.; Ouali, A.; Guerin, M.; Cernák, J.; Chomic, J. *Inorg. Chim. Acta* **1988**, *147*, 189.
- (33) (a) Range, K. J.; Kühnel, S.; Zabel, M. *Acta Crystallogr.* **1989**, *C45*, 1419. (b) Range, K. J.; Zabel, M.; Meyer, H.; Fischer, H. Z. *Naturforsch.* **1985**, *40B*, 618. (c) Zabel, M.; Kühnel, S.; Range, K. J. *Acta Crystallogr.* **1989**, *C45*, 1619.

- (34) (a) Hoskins, B. F.; Robson, R.; Scarlett, N. V. Y. *J. Chem. Soc., Chem. Commun.* **1994**, 2025. (b) Sakaguchi, U.; Tomioka, K.; Yoneda, H. *Inorg. Chim. Acta* **1985**, *101*, 23. (c) Cernák, J.; Gérard, F.; Chomic, J. *Acta Crystallogr.* **1993**, *C49*, 1294. (d) Omary, M. A.; Webb, T. R.; Assefa, Z.; Shankle, G. E.; Patterson, H. H. *Inorg. Chem.* **1998**, *37*, 1380. (e) Shek, I. P. Y.; Wong, W.-Y.; Lau, T.-C. *New J. Chem.* **2000**, *24*, 733. (f) Iwamoto, T. In *Comprehensive Supramolecular Chemistry*; Lehn, J. M., Atwood, J. L., Davies, J. E. D., MacNicol, D. D., Vögtle, F., Alberti, G., Bein, T., Eds.; Pergamon Press: Oxford, 1996; Vol. 7, pp 681 and references therein.
- (35) Leznoff, D. B.; Rancurel, C.; Sutter, J.-P.; Rettig, S. J.; Pink, M.; Paulsen, C.; Kahn, O. *J. Chem. Soc., Dalton Trans.* **1999**, 3593.
- (36) Kahn, O. *Molecular Magnetism*; VCH: Weinheim, 1993.

Table 1. Comparison of Cyanide (ν_{CN}) Absorptions (cm^{-1}) for Complexes **1–5** and Related Systems

complex	ν_{CN} absorption(s)
K[Au(CN) ₂]	2141 ⁴⁴
[Cu(cyclen)Au(CN) ₂][Au(CN) ₂]	2177, 2138 ²⁸
Cu(pyrazine)[Au(CN) ₂] ₂	2209, 2158 ^{26,28}
[Ni(tren)Au(CN) ₂][Au(CN) ₂]	2179, 2144 ²⁷
[Cu(tren)Au(CN) ₂][Au(CN) ₂] (1)	2205, 2153, 2141
[Cu(en) ₂ Au(CN) ₂][Au(CN) ₂] (2)	2143
Cu(dien)[Au(CN) ₂] (3)	2195, 2143
Cu(tmeda)[Au(CN) ₂] (4)	2191, 2174, 2152 ²⁵
Cu(tmeda)[Au(CN) ₂] _{1.5} (ClO ₄) _{0.5} (5)	2199, 2168

reaction solution as purple/blue crystals suitable for X-ray structural analysis. Yield: 0.059 g (86%). Anal. Calcd for C₈H₁₆N₈Au₂Cu: C, 14.09; H, 2.37; N, 16.44. Found: C, 14.13; H, 2.37; N, 16.38. IR (KBr): 2143 (ν_{CN}), 1584, 1263, 1022, 972, 702 cm^{-1} .

Cu(dien)[Au(CN)₂] (3**).** To a 10 mL aqueous solution of Cu(ClO₄)₂·6H₂O (0.037 g, 0.1 mmol) was added a 2 mL aqueous solution of dien (stock solution, 0.1 mmol). A 2 mL aqueous solution of KAu(CN)₂ (0.059 g, 0.2 mmol) was added dropwise with stirring to this dark blue solution, resulting in an immediate blue precipitate, which was filtered and air-dried to give Cu(dien)[Au(CN)₂]₂ (**3**). The filtrate was covered and cooled overnight to yield X-ray quality crystals of **3**. The crystals and powder had identical IR spectra. Yield: 0.051 g (77%). Anal. Calcd for C₈H₁₃N₇Au₂Cu: C, 14.46; H, 1.97; N, 14.75. Found: C, 14.48; H, 1.91; N, 14.63. IR (KBr): 2195 (ν_{CN}), 2143 (ν_{CN}), 1582, 1460, 1310, 1250, 1088, 1026, 956, 820, 638 cm^{-1} .

Cu(tmeda)[Au(CN)₂]_{1.5}(ClO₄)_{0.5} (5**).** To a 10 mL aqueous solution of Cu(ClO₄)₂·6H₂O (0.037 g, 0.1 mmol) was added a 2 mL aqueous solution of tmeda (stock solution 0.1 mmol). A 2 mL aqueous solution of KAu(CN)₂ (0.043 g, 0.15 mmol) was added dropwise to this blue solution, resulting in an immediate blue precipitate, which was filtered and air-dried to give Cu(tmeda)[Au(CN)₂]_{1.5}(ClO₄)_{0.5} (**5**). Yield: 0.046 g (76%). Anal. Calcd for C₁₈H₃₂N₁₀Au₃ClCu₂O₄: C, 17.93; H, 2.67; N, 11.61. Found: C, 17.78; H, 2.67; N, 11.41. IR (KBr): 2199 (ν_{CN}), 2168 (ν_{CN}), 1468, 1286, 1109, 1018, 997, 951, 808, 768, 625 cm^{-1} . Single crystals were prepared by slow diffusion of aqueous solutions of Cu(II)/tmeda and KAu(CN)₂ in an H-shaped tube. The crystals and powder had comparable IR data. Changing the Cu:Au stoichiometry in the reaction to 1:2 yields Cu(tmeda)[Au(CN)₂]₂ (**4**).²⁵

X-ray Crystallographic Analysis. [Cu(tren)Au(CN)₂][Au(CN)₂] (**1**) and Cu(dien)[Au(CN)₂]₂ (**3**). Crystallographic data for all structures are collected in Table 2. A blue prism of **1** having dimensions 0.23 × 0.09 × 0.06 mm was mounted on a glass fiber using epoxy adhesive. Data in the range 4° ≤ 2θ ≤ 52° were recorded using the diffractometer control program DIFRAC³⁷ and an Enraf Nonius CAD4F diffractometer. The data were corrected by integration for the effects of absorption (transmission range: 0.194–0.400). Data reduction included corrections for Lorentz and polarization effects. Final unit-cell dimensions were determined from 50 well-centered reflections in the range 38° ≤ 2θ ≤ 47°.

Coordinates and anisotropic displacement parameters for the non-hydrogen atoms were refined. Hydrogen atoms were placed in calculated positions ($d(\text{C}-\text{H})$ 0.95 Å; $d(\text{N}-\text{H})$ 0.93 Å), and their coordinate shifts were linked with those of the respective carbon or nitrogen atoms during refinement. Isotropic thermal parameters for the hydrogen atoms were initially assigned proportionately to the equivalent isotropic thermal parameters of their respective carbon or nitrogen atoms. Subsequently the isotropic thermal parameters for the C–H hydrogen atoms were constrained to have identical shifts during refinement, as were those for the N–H hydrogen atoms. An extinction parameter³⁸ was included in the final cycles of full-matrix least-squares refinement of 193 parameters for 1729 data ($I_o \geq 2.5\sigma(I_o)$). Selected bond lengths and angles for **1** are found in Table 3.

For **3**, data were collected on a Rigaku/ADSC CCD diffractometer as described below. The structure solution and refinement procedure was analogous to that for **1**. Coordinates for the non-hydrogen atoms

of **3** were refined. Anisotropic displacement parameters were refined for the Au and Cu atoms. Hydrogen atoms were placed in calculated positions ($d(\text{C}-\text{H})$ 0.95 Å; $d(\text{N}-\text{H})$ 0.93 Å), and their coordinate shifts were linked with those of the respective carbon or nitrogen atoms during refinement. Isotropic thermal parameters for the hydrogen atoms were initially assigned proportionately to the isotropic thermal parameters of their respective carbon or nitrogen atoms. Subsequently the isotropic thermal parameters for all hydrogen atoms were constrained to have identical shifts during refinement. The Flack enantiopole parameter³⁹ (0.628(18)) was included the final cycles of full-matrix least-squares refinement of 177 parameters for 3316 data ($I_o \geq 2.0\sigma(I_o)$). Selected bond lengths and angles for **3** are found in Table 5.

The programs used for absorption corrections, data reduction, and structure solution of **1** and **3** and all graphical output were from the NRCVAX Crystal Structure System.⁴⁰ The structures were refined using CRYSTALS.⁴¹ Complex scattering factors for neutral atoms⁴² were used in the calculation of structure factors.

[Cu(en)₂Au(CN)₂][Au(CN)₂] (2**) and Cu(tmeda)[Au(CN)₂]_{1.5}(ClO₄)_{0.5} (**5**).** A blue block crystal of **2** having dimensions of 0.30 × 0.15 × 0.15 mm (0.30 × 0.15 × 0.08 mm for **5**) was mounted on a glass fiber and measured on a Rigaku/ADSC CCD diffractometer. Data were collected in 0.50° oscillations with 35.0 s (46.0 s for **5**) exposures to a maximum 2θ value of 55.6° (55.7° for **5**). A sweep of data was done using φ oscillations from 0.0 to 190.0° at χ = −90°, and a second sweep was performed using ω oscillations between −19.0 and 23.0° at χ = −90°. The final unit-cell parameters were obtained by least squares on the setting angles for 2262 reflections with 2θ = 7.2–55.6° (12967 reflections with 2θ = 6.2–55.8° for **5**). The data for **2** (3130 data collected, 777 unique; $R_{\text{int}} = 0.038$) and for **5** (20031 data collected, 3579 unique; $R_{\text{int}} = 0.071$) were processed and corrected for Lorentz and polarization effects and absorption (minimal/maximal transmission 0.4391–1.0000 for **2**, 0.5244–1.0000 for **5**).⁴³

The structures were solved by direct methods (SIR97) and expanded using Fourier techniques (data/parameter ratio: 19.73 for **2**, 12.74 for **5**). Full-matrix least-squares refinement was conducted with all non-hydrogen atoms anisotropic; hydrogen atoms were either refined isotropically (**2**) or not refined (**5**). For **2**, final $R = 0.066$, $R_w = 0.074$, GOF = 1.23 on all data and $R = 0.030$, $R_w = 0.036$ on 681 observed reflections ($I_o > 3\sigma(I_o)$). For **5**, final $R = 0.071$, $R_w = 0.088$, GOF = 0.80 on all data and $R = 0.033$, $R_w = 0.040$ on 2715 observed reflections ($I > 3\sigma(I)$). Selected bond lengths and angles are found in Table 4 for **2** and Table 6 for **5**.

Results

Synthesis. The reaction of an aqueous solution of Cu(ClO₄)₂·6H₂O containing 1 or 2 equiv of capping amine ligand with an aqueous solution of K[Au(CN)₂] produced a product upon slow evaporation or cooling of the resulting solution (**1** and **2**) or an immediate precipitate of polymeric product (**3–5**). The capping ligands used can occupy four (tren), three (dien), or two (en, tmeda) coordination sites on the Cu(II) center (Scheme 1), leaving progressively more sites available for *N*-cyanide binding upon shifting from tren to tmeda. IR spectra of all complexes are invaluable in determining whether the cyanide-nitrogen donors have bound to the Cu(II) center; a blue-shift from the value of free [Au(CN)₂][−] (2141 cm^{-1})⁴⁴ indicates an

(38) Larson, A. C. In *Crystallographic Computing*; Ahmed, F. R., Ed.; Munksgaard: Copenhagen, 1970; p 291.

(39) Flack, H. *Acta Crystallogr.* **1983**, A39, 876.

(40) Gabe, E. J.; LePage, Y.; Charland, J.-P.; Lee, F. L.; White, P. S. J. *Appl. Crystallogr.* **1989**, 22, 384.

(41) Watkin, D. J.; Prout, C. K.; Caruthers, J. R.; Betteridge, P. W.; Cooper, R. I. CRYSTALS Issue 11, Chemical Crystallography Laboratory, University of Oxford, Oxford, England, 1999.

(42) (a) *International Tables for X-ray Crystallography*; Kynoch Press: Birmingham, U.K. (present distributor Kluwer Academic Publishers: Boston, MA), 1975; Vol. IV, p 99.

(43) *d*TREK: Area Detector Software*; Molecular Structure Corp.: The Woodlands, TX, 1997.

(44) Jones, L. H.; Penneman, R. A. *J. Chem. Phys.* **1954**, 22, 965.

(37) Gabe, E. J.; White, P. S.; Enright, G. D. *DIFRAC A Fortran 77 Control Routine for 4-Circle Diffractometers*; N.R.C.: Ottawa, 1995.

Table 2. Summary of Crystallographic Data

	1^a	2^b	3^b	5^b
formula	C ₁₀ H ₁₈ N ₈ Au ₂ Cu	C ₈ H ₁₆ N ₈ Au ₂ Cu	C ₈ H ₁₃ Au ₂ CuN ₇	C ₉ H ₁₆ N ₅ Au _{1.5} Cu _{0.5} O ₂
fw	707.78	681.75	664.71	602.98
space group	<i>P</i> 2 ₁ / <i>n</i> (No. 14)	<i>C</i> 2/ <i>m</i> (No. 12)	<i>I</i> c (No. 9)	<i>R</i> 32 (No. 155)
<i>a</i> , Å	7.3640(20)	10.5638(6)	12.447(2)	13.1465(4)
<i>b</i> , Å	13.5538(20)	13.0914(7)	17.569(3)	13.1465(4)
<i>c</i> , Å	17.121(3)	6.2810(4)	14.040(2)	48.048(1)
α, deg	90	90	90	90
β, deg	93.909(21)	119.962(4)	112.86(2)	90
γ, deg	90	90	90	120
<i>V</i> , Å ³	1704.8	752.54	2829.1	7191.6
<i>Z</i>	4	2	8	18
ρ _{calc} , g/cm ³	2.758	3.01	3.121	2.51
μ, cm ⁻¹	183.7	209.15	221.2	152.02
<i>T</i> (K)	293	198	173	173
<i>R</i> , <i>R</i> _w (<i>I</i> _o > <i>xσ</i> (<i>I</i> _o)) ^{c,d,e}	0.031, 0.026 ^c	0.030, 0.036 ^d	0.046, 0.051 ^e	0.033, 0.040 ^d
<i>R</i> , <i>R</i> _w (all data)		0.066, 0.074		0.071, 0.088

^a Enraf-Nonius CAD-4 diffractometer, Mo Kα radiation ($\lambda = 0.71069$ Å), graphite monochromator. ^b Rigaku/ADSC CCD diffractometer, detector swing angle -5.5° , aperture 94.0×94.0 mm at a distance of 40.52 mm from the crystal, Mo Kα radiation ($\lambda = 0.71069$ Å), graphite monochromator. ^c $x = 2.5$. Function minimized $\sum w(|F_o| - |F_c|)^2$ where $w^{-1} = \sigma^2(F_o) + 0.0001F_o^2$, $R = \sum ||F_o| - |F_c|| / \sum |F_o|$, $R_w = (\sum w(|F_o| - |F_c|)^2 / \sum w|F_o|^2)^{1/2}$. ^d $x = 3$. Function minimized $\sum w(|F_o^2 - F_c^2|)^2$ where $w^{-1} = \sigma^2(F_o^2)$, $R = \sum ||F_o| - |F_c|| / \sum |F_o|$, $R_w = (\sum w(|F_o| - |F_c|)^2 / \sum w|F_o|^2)^{1/2}$. ^e $x = 2$. Function minimized $\sum w(|F_o| - |F_c|)^2$ using robust-resistant weighting:⁷⁰ $w = [12.9t_0(|F_c|/|F_{c,max}) - 6.85t_1(|F_c|/|F_{c,max}) + 11.2t_2(|F_c|/|F_{c,max})]^{-1} [1 - ((|F_o| - |F_c|)/(6\Delta F_{est}))^2]^2$, t_n are the polynomial functions of the Chebyshev series, and ΔF_{est} is estimated from the Chebyshev fitting.⁷¹ Five reflections having $(|F_o| - |F_c|) \geq |6\Delta F_{est}|$ were assigned $w = 0$.

Table 3. Selected Bond Lengths (Å) and Angles (deg) for [Cu(tren)Au(CN)₂][Au(CN)₂] (**1**)

Au(1)–C(11)	1.962(13)	Au(1)–C(12)	1.991(14)
Au(2)–C(21)	1.982(12)	Au(2)–C(22)	1.992(12)
Cu(1)–N(1)	2.126(10)	Cu(1)–N(4)	2.039(8)
Cu(1)–N(7)	2.039(9)	Cu(1)–N(10)	2.040(10)
Cu(1)–N(21)	1.950(9)	N(11)–C(11)	1.143(17)
N(12)–C(12)	1.107(18)	N(21)–C(21)	1.129(15)
N(22)–C(22)	1.118(15)		
C(11)–Au(1)–C(12)	176.0(5)	C(21)–Au(2)–C(22)	179.4(5)
N(1)–Cu(1)–N(4)	83.7(4)	N(1)–Cu(1)–N(7)	113.3(4)
N(1)–Cu(1)–N(10)	111.8(4)	N(1)–Cu(1)–N(21)	99.6(4)
N(4)–Cu(1)–N(7)	84.1(4)	N(4)–Cu(1)–N(10)	84.8(4)
N(4)–Cu(1)–N(21)	176.1(4)	N(7)–Cu(1)–N(10)	131.8(4)
N(7)–Cu(1)–N(21)	96.4(4)	N(10)–Cu(1)–N(21)	92.0(4)
Cu(1)–N(21)–C(21)	169.8(10)		

Table 4. Selected Bond Lengths (Å) and Angles (deg) for [Cu(en)₂Au(CN)₂][Au(CN)₂] (**2**)

Au(1)–Au(2)	3.1405(2)	Au(1)–C(1)	1.982(7)
Au(1)–C(2)	1.986(8)	Cu(1)–N(1)	2.576(6)
Cu(1)–N(3)	2.013(4)	N(1)–C(1)	1.134(9)
C(3)–C(3') ^a	1.51(1)	N(3)–C(3)	1.469(7)
N(3)–C(3)	1.469(7)		
C(1)–Au(1)–C(1') ^b	180.0	C(2)–Au(2)–C(2') ^c	180.0
Au(2)–Au(1)–Au(2') ^b	180.0	Au(2)–Au(1)–C(1)	98.8(2)
Au(2)–Au(1)–C(1') ^b	81.2(2)	Au(1)–Au(2)–C(2)	90.0
Au(1)–C(1)–N(1)	176.1(6)	Au(2)–C(2)–N(2)	180.0
Cu(1)–N(1)–C(1)	138.6(5)	N(3)–Cu(1)–N(3') ^d	180.0
N(3)–Cu(1)–N(3') ^e	95.7(3)	N(3)–C(3)–C(3') ^a	106.4(4)
Cu(1)–N(3)–C(3)	107.9(3)		

^{a–e} Symmetry transformations: ^a1 – *x*, *y*, –*z*; ^b2 – *x*, –*y*, 2 – *z*; ^c2 – *x*, –*y*, 1 – *z*; ^d1 – *x*, –*y*, –*z*; ^e*x*, –*y*, *z*.

Au(I)–Cu(II) bridging cyanide. Similarly, the absence of any bands corresponding to the perchlorate anion in the IR spectra of all the products (except for **5**, see below) confirmed the total replacement of two ClO₄[–] anions by two [Au(CN)₂][–] units. The ν_{CN} bands in the IR spectra of each complex are collected in Table 1 for comparison. The crystal structures of the complexes described below, presented in order of increasing number of available open coordination sites, show a wide range of supra-molecular geometries and are influenced strongly by aurophilic interactions.

Table 5. Selected Bond Lengths (Å) and Angles (deg) for Cu(dien)[Au(CN)₂]₂ (**3**)

Au(1')–Au(2') ^a	3.3276(21)	Au(2)–Au(3'') ^a	3.3586(19)
Au(3'')–Au(4)	3.3626(22)	Au(1)–C(101)	1.967(15)
Au(1)–C(102)	2.001(16)	Au(2)–C(201)	2.002(17)
Au(2)–C(202)	1.986(17)	Au(3)–C(301)	1.998(18)
Au(3)–C(302)	1.991(16)	Au(4)–C(401)	1.976(16)
Au(4)–C(402)	1.995(17)	Cu(1)–N(11)	2.000(19)
Cu(1)–N(14)	2.016(11)	Cu(1)–N(17)	1.981(18)
Cu(1)–N(101)	1.995(13)	Cu(1)–N(402)	2.352(15)
Cu(2)–N(21)	2.014(13)	Cu(2)–N(24)	1.997(13)
Cu(2)–N(27)	2.030(13)	Cu(2)–N(202)	2.375(19)
Cu(2)–N(301)	1.980(15)	N(101)–C(101)	1.139(20)
N(102)–C(102)	1.115(22)	N(201)–C(201)	1.123(23)
N(202)–C(202)	1.144(22)	N(301)–C(301)	1.119(23)
N(302)–C(302)	1.125(23)	N(401)–C(401)	1.128(22)
N(402)–C(402)	1.111(23)		
C(101)–Au(1)–C(102)	175.9(8)	C(201)–Au(2)–C(202)	174.5(7)
C(301)–Au(3)–C(302)	175.7(6)	C(401)–Au(4)–C(402)	174.5(8)
Au(1')–Au(2)–Au(3')	150.86(7)	Au(2)–Au(3'')–Au(4)	145.62(7)
N(11)–Cu(1)–N(14)	84.4(6)	N(11)–Cu(1)–N(17)	157.7(5)
N(11)–Cu(1)–N(101)	96.3(7)	N(11)–Cu(1)–N(402)	94.8(7)
N(14)–Cu(1)–N(17)	84.0(6)	N(14)–Cu(1)–N(101)	176.7(5)
N(14)–Cu(1)–N(402)	88.4(5)	N(17)–Cu(1)–N(101)	96.4(6)
N(17)–Cu(1)–N(402)	103.9(7)	N(101)–Cu(1)–N(402)	88.3(5)
N(21)–Cu(2)–N(24)	84.5(6)	N(21)–Cu(2)–N(27)	162.4(6)
N(21)–Cu(2)–N(202)	94.0(6)	N(21)–Cu(2)–N(301)	96.3(6)
N(24)–Cu(2)–N(27)	84.6(6)	N(24)–Cu(2)–N(202)	88.0(6)
N(24)–Cu(2)–N(301)	176.8(7)	N(27)–Cu(2)–N(202)	99.4(6)
N(27)–Cu(2)–N(301)	93.8(6)	N(202)–Cu(2)–N(301)	94.9(6)
Cu(1)–N(101)–C(101)	168.8(14)	Cu(1)–N(402)–C(402)	137.0(13)
Cu(2)–N(301)–C(301)	173.5(18)	Cu(2)–N(202)–C(202)	137.1(17)

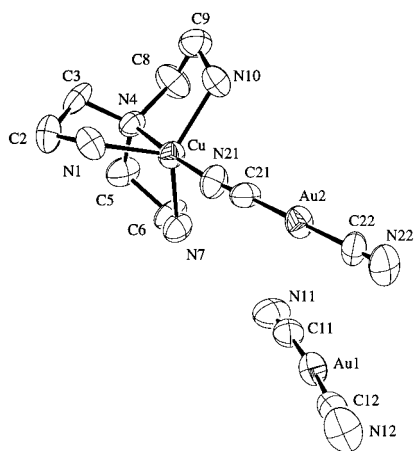
^a Symmetry transformations: (') *x*, 1 – *y*, –1/2 + *z*; (') *x*, 1 – *y*, 1/2 + *z*.

Structural Studies. [Cu(tren)Au(CN)₂][Au(CN)₂] (**1**). The addition of 2 equiv of K[Au(CN)₂] to an aqueous solution of Cu(II)/tren yields crystals of Cu(tren)[Au(CN)₂]₂ (**1**) by slow evaporation of the resulting solution. The IR data, showing three ν_{CN} bands at 2205, 2157, and 2141 cm⁻¹, suggested that at least one [Au(CN)₂][–] unit was acting as a ligand (high-energy bands) and one [Au(CN)₂][–] anion was free (2141 cm⁻¹). Confirming this, the X-ray crystal structure of **1** (Figure 1) revealed an ionic system of the form [Cu(tren)Au(CN)₂][Au(CN)₂]. The cationic Cu(II) center in **1** has a five-coordinate, distorted trigonal pyramidal geometry, with one tren and one N-bound dicyanoau-

Table 6. Selected Bond Lengths (Å) and Angles (deg) for Cu(tmeda)[Au(CN)₂]_{1.5}(ClO₄)_{0.5} (**5**)

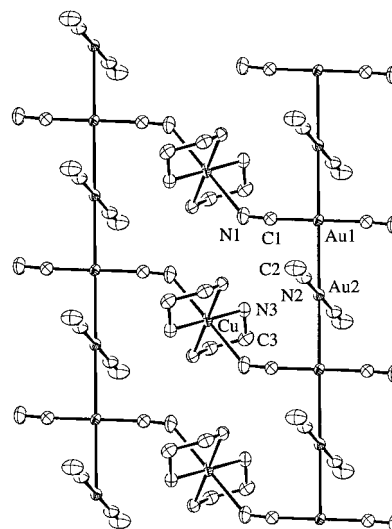
Au(1)–Au(1') ^a	3.5949(8)	Au(1'')–Au(2) ^b	3.4018(7)
Au(1)–C(8)	1.97(1)	Au(1)–C(9') ^c	1.96(1)
Au(2)–C(7)	2.00(1)	Cu(1)–N(1)	2.090(9)
Cu(1)–N(2)	2.036(9)	Cu(1)–N(3)	2.010(9)
Cu(1)–N(4)	2.152(9)	Cu(1)–N(5)	1.961(9)
N(1)–C(1)	1.48(1)	N(1)–C(2)	1.51(1)
N(1)–C(3)	1.47(1)	N(2)–C(4)	1.47(1)
N(2)–C(5)	1.49(1)	N(2)–C(6)	1.47(1)
N(3)–C(7)	1.14(1)	N(4)–C(8)	1.16(1)
N(5)–C(9)	1.16(1)	C(3)–C(4)	1.52(1)
C(8)–Au(1)–C(9') ^c	179.7(4)	C(7)–Au(2)–C(7') ^d	177.7(7)
Au(1)–C(8)–N(4)	176.4(9)	Au(2)–C(7)–N(3)	176(1)
Au(1)–C(9)–N(5)	177.0(9)	N(1)–Cu(1)–N(2)	84.6(4)
N(1)–Cu(1)–N(3)	161.0(4)	N(1)–Cu(1)–N(4)	100.0(4)
N(1)–Cu(1)–N(5)	90.9(4)	N(2)–Cu(1)–N(3)	92.4(4)
N(2)–Cu(1)–N(4)	94.3(3)	N(2)–Cu(1)–N(5)	170.2(4)
N(3)–Cu(1)–N(4)	98.9(4)	N(3)–Cu(1)–N(5)	89.0(4)
N(4)–Cu(1)–N(5)	95.1(4)	Cu(1)–N(3)–C(7)	162(1)
Cu(1)–N(4)–C(8)	158.8(9)	Cu(1)–N(5)–C(9)	173.6(9)

^{a-d} Symmetry transformations: ^a2 – y, x – y, z; ^b2 – x, 1 – x + y, 1 – z; ^c1 + y, x, –z; ^dy, x, –z.

**Figure 1.** Molecular structure of [Cu(tren)Au(CN)₂][Au(CN)₂] (**1**) (ORTEP, 50% ellipsoids).

rate completing the coordination sphere. The charge on this monocation is balanced by a free [Au(CN)₂][–] anion; both dicyanoaurate units have nearly linear geometries. Importantly, there are no significant gold–gold interactions in **1**. The sum of the van der Waals radii of two Au(I) centers is 3.60 Å and is thus considered to be the upper limit of a distance for a viable auriphilic interaction.^{12,45} The Au(1)⋯Au(2) distance of 3.6067–(12) Å is beyond this threshold, and the Au(2)⋯Au(2') distance (to the next molecular unit, symmetry 1 – x, 1 – y, 1 – z) of 3.7893(12) Å is even larger. This situation is quite different from the [Cu(cyclen)Au(CN)₂][Au(CN)₂] system, in which the [Cu(cyclen)Au(CN)₂] cations form dimers via auriphilic interactions of 3.162(2) Å, as do the free [Au(CN)₂][–] anions (3.264 Å).²⁸ Substituting Cu(II) for Ni(II) yields the related [Ni(tren)Au(CN)₂][Au(CN)₂] system, which contains a 1-D coordination polymer that interacts with free [Au(CN)₂][–] anions by auriphilic interactions to yield a 2-D system.²⁷

[Cu(en)₂Au(CN)₂][Au(CN)₂] (2). Crystals of Cu(en)₂[Au(CN)₂]₂ (**2**) formed upon slow evaporation of a saturated aqueous solution of **2**. Only one ν_{CN} band at 2143 cm^{–1} was observed, close to the value found for K[Au(CN)₂]. The X-ray crystal structure of **2** revealed a two-dimensional array of [Cu(en)₂]²⁺

**Figure 2.** Extended structure of [Cu(en)₂Au(CN)₂][Au(CN)₂] (**2**) viewed perpendicular to the *ac* plane (ORTEP, 50% ellipsoids).

cations and [Au(CN)₂][–] anions (Figure 2) in the *ac* plane, arranged in 1-D-chains of [Au(CN)₂][–] anions cross-linked by 1-D chains of [(en)₂Cu–NCAuCN]⁺ units. The Cu(II) center in **2** has a tetragonally distorted octahedral geometry, with the en ligands bound in the equatorial plane. The Jahn–Teller elongated axial Cu–N(1) distance is 2.576(6) Å, similar to lengthened distances in many other Cu(II) octahedral systems.^{46–48} This axial *N*-cyanide binding generates 1-D chains in the *a* direction.

The [Au(CN)₂][–] anions in **2** form a linear 1-D chain of [Au(CN)₂][–] units along the *c* axis via auriphilic interactions; the Au(1)–Au(2) bond length is a short 3.1405(2) Å. Adjacent units are staggered at nearly right angles to each other (85.3°). This angle has been found to become more eclipsed with increasing Au–Au bond length,⁴⁹ as illustrated by the 23.3° torsion angle between non-interacting [Au(CN)₂][–] units in **1**. The closest Au⋯Au distance between chains is 8.41 Å. Both one-²⁰ and two-dimensional^{18,19,29} associations of dicyanoaurate units have been previously observed. The tetrameric [Au(CN)₂][–] units in [16-pyrimidinium crown-4][Au(CN)₂]₄·6.5H₂O²⁰ have bond lengths of 3.128(3), 3.220(4), and 3.274(5) Å and torsion angles between 13.7° and 59.3°; hence the Au–Au bond length in **2** is quite short.

Thus, auriphilic interactions play a dominant role in defining the solid-state structure of **2**. They overcome electrostatic interactions, which would normally preclude the anionic [Au(CN)₂][–] units from associating in the observed [– – –] arrangement. Other unexpected electrostatic sequences, such as [+ – – +],⁵⁰ [– + + –],^{51,52} and [+ neutral –],⁵³ have been reported in various ionic gold(I) complexes.

Cu(dien)[Au(CN)₂]₂ (3). Addition of 2 equiv of K[Au(CN)₂] to an aqueous solution of Cu(II)/dien causes the immediate

(45) Bardají, M.; Laguna, A. *J. Chem. Educ.* **1999**, *76*, 201.

- (46) Hathaway, B. J. In *Comprehensive Coordination Chemistry*; Wilkinson, G., Gill, R. D., McCleverty, J. A., Eds.; Pergamon: Oxford, 1987; Vol. 5, p 533.
- (47) Kou, H.-Z.; Wang, H.-M.; Liao, D.-Z.; Cheng, P.; Jiang, Z.-H.; Yan, S.-P.; Huang, X.-Y.; Wang, G.-L. *Aust. J. Chem.* **1998**, *51*, 661.
- (48) Yuge, H.; Iwamoto, T. *J. Chem. Soc., Dalton Trans.* **1994**, 1237.
- (49) Pathaneni, S. S.; Desiraju, G. R. *J. Chem. Soc., Dalton Trans.* **1993**, 319.
- (50) Bauer, A.; Schmidbaur, H. *J. Am. Chem. Soc.* **1996**, *118*, 5324.
- (51) Adams, H.-N.; Hiller, W.; Strähle, J. *Z. Anorg. Allg. Chem.* **1982**, *485*, 81.
- (52) Conzelmann, W.; Hiller, W.; Strähle, J. *Z. Anorg. Allg. Chem.* **1984**, *512*, 169.
- (53) Yip, J. H. K.; Feng, R.; Vittal, J. J. *Inorg. Chem.* **1999**, *38*, 3586.

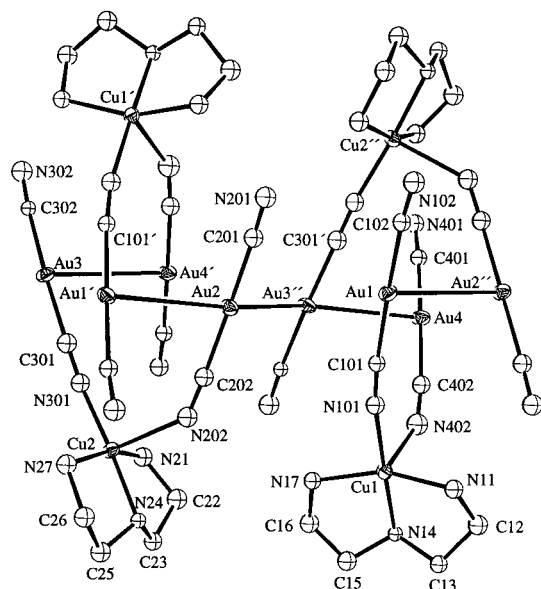


Figure 3. Extended structure of $\text{Cu}(\text{dien})[\text{Au}(\text{CN})_2]_2$ (**3**) (ORTEP, 50% ellipsoids).

precipitation of $\text{Cu}(\text{dien})[\text{Au}(\text{CN})_2]_2$ (**3**), which exhibits two ν_{CN} bands at 2195 and 2143 cm^{-1} . The X-ray crystal structure (Figure 3) revealed a 1-D system, based on an asymmetric unit containing two crystallographically distinct $\text{Cu}(\text{dien})[\text{Au}(\text{CN})_2]$ – $[\text{Au}(\text{CN})_2]$ units. Each Cu(II) center in **3** has an irregular square pyramidal geometry, with the dien and one N-bound cyanide ligand in the basal plane and a weakly N-bound cyanide in the apical site. The $\text{Cu}(\text{dien})[\text{Au}(\text{CN})_2]_2$ moieties interconnect via aurophilic interactions to yield a kinked chain of tetrameric Au units which propagate in the c direction. Each $[\text{Au}(\text{CN})_2]^-$ unit in a tetramer is bound to a different Cu(dien) moiety; thus no $[\text{Au}(\text{CN})_2]^-$ unit bridges two Cu(II) centers (one end is always unbound). The Au–Au bonds within the tetramer are 3.3276(21), 3.3586(19), and 3.3626(22) Å for Au(1')–Au(2), Au(2)–Au(3''), and Au(3'')–Au(4), respectively. As all Au–Au distances between tetrameric units are greater than 4 Å, there is a clear structural break between the gold atoms of each tetramer. Within each tetramer, the gold atoms lie on a zigzag line as indicated by the Au(1')–Au(2)–Au(3'') and Au(2)–Au(3'')–Au(4) bond angles of 150.86(7)° and 145.62(7)°. The two central $[\text{Au}(\text{CN})_2]^-$ units themselves are nearly eclipsed, with a C(201)–Au(2)–Au(3'')–C(301') torsion angle of only 1.6°, but the outer $[\text{Au}(\text{CN})_2]^-$ units are staggered by 48.7° (C(101')–Au(1')–Au(2)–C(201)) and –53.5° (C(301')–Au(3'')–Au(4)–C(401)) with respect to the central pair.

Aurophilicity-generated gold(I) tetramer motifs have been observed in homometallic Au(I) systems. For example, [24-pyrimidinium crown-6][$\text{Au}(\text{CN})_2$] $_4(\text{NO}_3)_2 \cdot 2\text{H}_2\text{O}$ and [16-pyrimidinium crown-4][$\text{Au}(\text{CN})_2$] $_4 \cdot 6.5\text{H}_2\text{O}$ both contain centrosymmetric zigzag “tetramers” of $[\text{Au}(\text{CN})_2]^-$ anions, with shorter, terminal Au–Au distances of 3.271(4) and 3.155(7) Å and longer central distances of 3.492(5) and 3.501(7) Å.²⁰ The central anions in both are essentially eclipsed, while the terminal ones are staggered 68.5° and 74.0° with respect to the central core. Both of these systems are more accurately described as containing pairs of interacting dimers; the unique tetramer in **3** has nearly equal central and terminal Au–Au bond lengths.

Cu(tmeda)[Au(CN)₂]₂ (4) and Cu(tmeda)[Au(CN)₂]_{1.5}(ClO₄)_{0.5} (5). The product that precipitates from solution upon the addition of $\text{K}[\text{Au}(\text{CN})_2]$ to an aqueous solution of Cu(II)/tmeda depends on the stoichiometric ratio of reactants used.

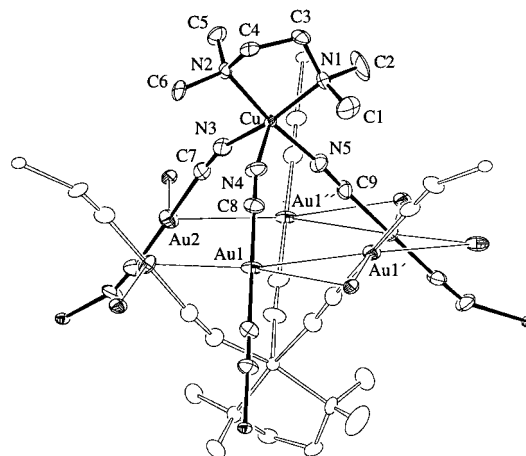


Figure 4. Extended structure of $\text{Cu}(\text{tmeda})[\text{Au}(\text{CN})_2]_{1.5}(\text{ClO}_4)_{0.5}$ (**5**) (ORTEP, 50% ellipsoids), showing two of three interpenetrating networks.

When the Cu:Au ratio is 1:2, $\text{Cu}(\text{tmeda})[\text{Au}(\text{CN})_2]_2$ (**4**) is obtained.²⁵ This compound consists of a 1-D coordinately bonded zigzag chain of $[(\text{tmeda})(\text{NCAuCN})\text{Cu}-\text{NCAuCN}-]$ units that assemble in a complex 3-D structure via aurophilic interactions of 3.3450(10) and 3.5378(8) Å. In addition to this being an excellent example of increasing dimensionality in heterometallic polymers via aurophilic interactions, **4** exhibits weak ferromagnetic interactions along the 1-D chain, likely mediated by the diamagnetic $[\text{Au}(\text{CN})_2]^-$ unit.

When the Cu:Au ratio is 2:3, a completely different product, of the form $\text{Cu}(\text{tmeda})[\text{Au}(\text{CN})_2]_{1.5}(\text{ClO}_4)_{0.5}$ (**5**), is isolated. The IR spectrum of **5** features two ν_{CN} bands at 2199 and 2168 cm^{-1} , suggesting that all the CN units in the complex are coordinated to a Cu(II) center. Indeed, the X-ray crystal structure of **5**, shown in Figure 4, revealed a polymeric, 2-D layered network. The Cu(II) center has a five-coordinate, distorted square pyramidal geometry, with one tmeda and two dicyanoaurate N atoms in the basal plane and one more N-bound cyanide in the apical position. Each $[\text{Au}(\text{CN})_2]^-$ unit bridges to another Cu(II) center, with approximate intrachain $\text{Cu}\cdots\text{Cu}$ distances of 10.2 Å. This generates a puckered, 2-D, honeycomb network of $\text{Cu}[\text{Au}(\text{CN})_2]_{1.5}$ units centered on the ab plane, which is sandwiched between insulating caps of Cu(II)-coordinated tmeda ligands (Figure 4). These layers, of approximately 16 Å width, are interspaced by uncoordinated ClO_4^- anions.

In fact there are *three* such networks interpenetrated in this layer, two of which are shown in Figure 4. A simplified, complete view of the interpenetrating network structure of **5**, viewed along c , is given in Figure 5a; the closest through-space $\text{Cu}\cdots\text{Cu}$ distance between networks is approximately 6.76 Å. Triply interpenetrating parallel 2-D networks are less common⁵⁴ than simpler double interpenetrating systems,⁵⁵ but what makes **5** particularly notable is that the three independent networks are *connected* by Au–Au bonds of 3.4018(7) and 3.5949(8) Å (Au(1'')–Au(2) and Au(1)–Au(1'), respectively). The gold atoms form a plane through the center of the $\text{Cu}[\text{Au}(\text{CN})_2]_{1.5}$

(54) (a) Liu, F.-Q.; Tilley, T. D. *Inorg. Chem.* **1997**, *36*, 5090. (b) Sharma, C. V. K.; Zaworotko, M. J. *Chem. Commun.* **1996**, 2655. (c) Zafar, A.; Yan, J.; Geib, S. J.; Hamilton, A. D. *Tetrahedron Lett.* **1996**, *37*, 2327. (d) Aoyama, T.; Endo, K.; Anzai, T.; Yamaguchi, Y.; Sawaki, T.; Kobayashi, K.; Kanehisa, N.; Hashimoto, H.; Kai, Y.; Masuda, H. *J. Am. Chem. Soc.* **1996**, *118*, 5562. (e) Fujita, M.; Kwon, Y. J.; Sasaki, O.; Yamaguchi, K.; Ogura, K. *J. Am. Chem. Soc.* **1995**, *117*, 7287.

(55) (a) Batten, S. R.; Robson, R. *Angew. Chem., Int. Ed.* **1998**, *37*, 1460. (b) Robson, R. *J. Chem. Soc., Dalton Trans.* **2000**, 3735.

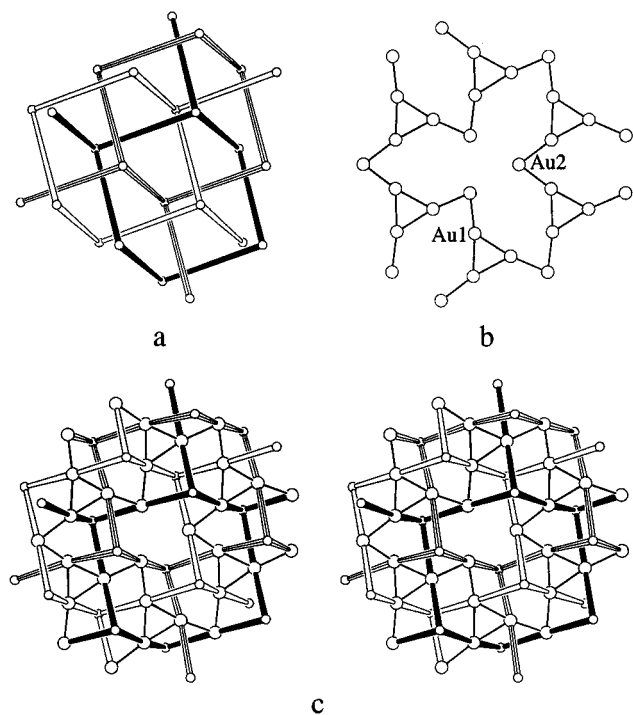


Figure 5. (a) The three interpenetrating networks of **5**, viewed approximately in the *c* direction, showing the Cu(II) centers. Tmeda ligands have been removed for clarity, and $[\text{Au}(\text{CN})_2]^-$ units are depicted as connecting rods. (b) Arrangement of Au(I) atoms in the central *ab* plane of the (tmeda)Cu[Au(CN) $_2$] $_{1.5}$ layer, viewed down the *c* axis. (c) Stereoview of **5**. Large and small circles represent Au(I) and Cu(II) centers, respectively.

layer, in which the Au(I) atoms arrange in triangles which are connected by Au(2) centers. The nonbonded Au(2) \cdots Au(2') and Au(1) \cdots Au(1'') distances are 4.782 and 4.116 Å, respectively. The 3-fold, symmetrical arrangement of gold centers in the *ab* plane is shown in Figure 5b and could also be described as a highly distorted close-packed 2-D array in which every fourth Au center is replaced by two Cu(II) centers, situated above and below the vacancy. Less complex hexagonal arrays of Au(I) and Ag(I) centers have been reported in $\text{M}[\text{Au}(\text{CN})_2]_3$ ($\text{M} = \text{Eu}, \text{Gd}, \text{Sm}$)²⁹ and KAgCO_3 .⁵⁶ A full stereoview of **5**, an amalgamation of the components shown in Figure 5a,b, is shown in Figure 5c.

Thus, although the 2-D structure of **5** is constructed from coordinate bond interactions, aurophilic interactions play an important role in defining the overall structure. Coordination polymers involving the $[\text{Au}(\text{CN})_2]^-$ unit have a propensity to display aurophilicity-supported interpenetration.^{26,28,30} Systems that incorporate $[\text{Ag}(\text{CN})_2]^-$ can also show extensive interpenetration.³¹

Interestingly, the 2-D layered system in **5** crystallizes in the chiral space group *R*32, despite the lack of chiral building blocks. Coordination polymers in chiral space groups are of interest as potential functional materials, and we are investigating NLO properties of **5** and related systems. There are fewer than 100 compounds that crystallize in this space group,⁵⁷ including five coordination polymers,⁵⁸ some of which have excellent NLO properties.^{58b} Bimetallic $[\text{Ni}(\text{N-methylethylenediamine})_2]_3\text{-}[\text{M}(\text{CN})_6]_2 \cdot n\text{H}_2\text{O}$ ($\text{M}(\text{III}) = \text{Fe}, \text{Co}$) are 2-D assemblies based on a honeycomb sheet structure, but there is no network interpenetration.²²

We recently reported that, in $\text{Cu}(\text{pyrazine})[\text{Au}(\text{CN})_2]_2$, the aurophilic interactions between interpenetrating nets appeared to augment the overall thermal stability of the system, an important requirement for useful functional materials.²⁶ The thermogravimetric analysis of **5** was thus examined. The TGA reveals that the network is stable only up to 160 °C, at which point a weight loss corresponding to the removal of the capping tmeda ligand occurs between 160 and 250 °C. At higher temperatures, the cyanide groups are lost in two steps, from 250 to 300 °C and from 340 to 370 °C. The tmeda ligand, which is not stabilized by aurophilic interactions, is lost at temperatures comparable to those observed in related systems, but the cyanide-loss temperatures are higher than those in $\text{K}_2\text{Zn}_3[\text{Fe}(\text{CN})_6]_2$.⁵⁹ It is possible that the gold–gold bonded network may give additional stability to **5**.

Magnetic Properties. The temperature (*T*) dependence of the molar magnetic susceptibility (χ_M) of polycrystalline samples of **1–5** was measured in the temperature range 2–300 K. For **1**, $\chi_M T = 0.44 \text{ cm}^3 \text{ K mol}^{-1}$ at 300 K and it exhibits Curie law behavior as the temperature is lowered to 2 K, consistent with isolated Cu(II), $S = 1/2$ centers.³⁶ This is in accordance with the ionic nature of **1**, in which there is no obvious pathway for magnetic exchange.

Despite the presence of 1-D chains linking Cu(II) centers in **2**, the chains are propagated via long axial *N*-cyanide bonds, significantly reducing potential magnetic interactions. At 300 K, $\chi_M T = 0.42 \text{ cm}^3 \text{ K mol}^{-1}$ and remains stable until 27 K, below which point it begins to drop until it reaches $0.36 \text{ cm}^3 \text{ K mol}^{-1}$ at 2 K. The magnetic susceptibility can be fitted with the Curie–Weiss law with $\theta = -0.38 \text{ K}$. Using the model for a 1-D Heisenberg chain of $S = 1/2$ centers,⁶⁰ an exchange coupling constant of $J = -0.17 \text{ cm}^{-1}$ with $g = 2.13$ is obtained. However, as this value is very low, other potential pathways, such as weak intermolecular hydrogen bonds, should also be considered. Hence the given *J* value should only be considered to be an approximation. In the closely related complex $[\text{Cu}(\text{en})_2\text{Ag}(\text{CN})_2][\text{Ag}(\text{CN})_2]$ (**2-Ag**),³² a low-temperature magnetic properties investigation (0.4–4.3 K) concluded that only weak magnetic interactions were present ($-J/k_B \ll 60 \text{ mK}$), propagated both within the chain and via a weak hydrogen-bonding network.

Similarly, for **3**, $\chi_M T = 0.46 \text{ cm}^3 \text{ K mol}^{-1}$ at 300 K and it exhibits Curie law behavior down to 10 K, below which a slight decrease is observed. The only potential pathway for magnetic exchange in **3** is via the Au–Au bonds. The ability of Au–Au bonds to propagate exchange interactions has not been probed up to this point, and this result may imply that they are poor mediators of magnetic exchange. The geometry of the aurophilic interactions vis-à-vis the Cu(II) magnetic centers may be a factor that helps determine the very weak interactions observed in **3**. An arrangement that provides larger magnetic orbital overlap³⁶ may permit aurophilic interactions to more effectively mediate magnetic exchange.

(58) (a) Su, C.-Y.; Kang, B.-S.; Yang, Q.-C.; Mak, T. C. W. *J. Chem. Soc., Dalton Trans.* **2000**, 1857. (b) Lin, W.; Wang, Z.; Ma, L. *J. Am. Chem. Soc.* **1999**, *121*, 11249. (c) Petrusenko, S. R.; Sieler, J.; Kokozay, V. N. *Z. Naturforsch.* **1997**, *52B*, 331. (d) Harrison, W. T. A.; Dussack, L. L.; Jacobson, A. J. *Inorg. Chem.* **1996**, *35*, 1461. (e) Cernák, J.; Chomic, J.; Kappenstein, C.; Dunaj-Jurco, M. *Z. Kristallogr.* **1994**, *209*, 430.

(59) (a) Cartraud, P.; Cointot, A.; Renaud, A. *J. Chem. Soc., Faraday Trans.* **1981**, *77*, 1561. (b) Chomic, J.; Cernák, J. *Thermochim. Acta* **1985**, *93*, 93.

(60) (a) Bonner, J. C.; Fisher, M. E. *Phys. Rev. A* **1964**, *135*, 646. (b) Hall, J. W.; Marsh, W. E.; Weller, R. R.; Hatfield, W. E. *Inorg. Chem.* **1981**, *20*, 1033.

(56) Jansen, M. *Angew. Chem., Int. Ed. Engl.* **1987**, *26*, 1098.

(57) Cambridge Structural Database, Version 2000.

Weak antiferromagnetic exchange is observed in **5**. For this 2-D system, at high temperatures $\chi_M T = 0.39 \text{ cm}^3 \text{ K mol}^{-1}$, consistent with noncorrelated $S = 1/2$ spins. As the temperature is lowered, the $\chi_M T$ value remains stable until 25 K, at which point it decreases to $0.32 \text{ cm}^3 \text{ K mol}^{-1}$ at 2 K, consistent with the presence of weak antiferromagnetic interactions. The magnetic susceptibility can be fitted with the Curie–Weiss law with $\theta = -0.34 \text{ K}$. Assuming that no significant magnetic interactions are propagated *between* interpenetrating networks,^{61,62} from a magnetic point of view, **5** can be considered as a 2-D honeycomb system in which each $S = 1/2$ center has three nearest neighbors in a tripodal arrangement. The data could be fitted to the theoretical expression for a 2-D Heisenberg honeycomb lattice⁶³ with best-fit values of $J = -0.13 \text{ cm}^{-1}$ and $g = 2.04$. Hence any internetwork magnetic interactions are clearly negligible. The J coupling, although weak, may in fact be a superposition of ferromagnetic and antiferromagnetic contributions. In the related $\text{Cu}(\text{tmeda})[\text{Au}(\text{CN})_2]_2$ system (**4**), a ferromagnetic interaction of $+2.34 \text{ cm}^{-1}$ was observed, mediated by diamagnetic $[\text{Au}(\text{CN})_2]^-$ units along a 1-D chain composed of alternating $\text{Cu}(\text{II})$ –basal/apical coordination in a $-\text{Cu}-\text{NC}-\text{Au}-\text{CN}-\text{Cu}-$ chain.²⁵ This basal/apical combination in $\text{Cu}(\text{II})$ complexes typically yields ferromagnetic coupling due to the effective orthogonality of the interacting $\text{Cu}(\text{II})$ magnetic orbitals.³⁶ In **5**, while a similar basal/apical pattern is present, there are also basal/basal connections which are expected to yield antiferromagnetic coupling.⁶⁴ The final observed magnetic behavior should be a synthesis of these two competing interactions in the 2-D array; hence the theoretical fit may not be a true representation of the magnetic structure of the system. In any case, it is clear that the diamagnetic $[\text{Au}(\text{CN})_2]^-$ units are mediating magnetic exchange between $\text{Cu}(\text{II})$ centers in **5**. Both ferro- and antiferromagnetic interactions between metal centers are mediated by the related dicyanamide anion (dca , $^-\text{N}(\text{CN})_2$) in $\text{M}(\text{dca})_2$ and $\text{M}(\text{dca})_2\text{L}_2$ systems ($\text{M} = \text{Mn}, \text{Fe}, \text{Co}, \text{Ni}, \text{Cu}$; $\text{L} = \text{pyridine}, \text{CH}_3\text{OH}, \text{CH}_3\text{CH}_2\text{OH}, \text{H}_2\text{O}, \text{DMF}$).⁶⁵ Weak magnetic interactions are also propagated by other diamagnetic cyanometalate anions, such as in $\text{Cu}(\text{en})_2[\text{Fe}(\text{CN})_5(\text{NO})]^{47}$ and $[\text{Ni}(\text{en})_2]_3[\text{Fe}(\text{CN})_6](\text{PF}_6)_2$.⁶⁶

Discussion

An examination of the structural trends in **1–5** in a global sense yields several observations. At first, as would be expected, increasing the number of uncapped, open sites for ligand coordination at the $\text{Cu}(\text{II})$ center increases structural dimensionality. Thus, **1** has one open site and is zero-dimensional, **2** and **3** have two open positions and are 2-D and 1-D, respec-

tively, and **4** and **5** have three open sites and are 3-D and 2-D, respectively. Of more interest is the increase in dimensionality or structural complexity that is attributable to aurophilic interactions. Clearly, Au–Au bonding plays an important role in determining the supermolecular structures of many of the compounds reported. $[\text{Cu}(\text{en})_2\text{Au}(\text{CN})_2][\text{Au}(\text{CN})_2]$ (**2**) is a 1-D coordination polymer, but aurophilic interactions increase the dimensionality to 2. Similarly, $\text{Cu}(\text{dien})[\text{Au}(\text{CN})_2]_2$ (**3**) is a molecular (0-D) system until aurophilic interactions are considered: the system is then properly described as a 1-D chain. $\text{Cu}(\text{tmeda})[\text{Au}(\text{CN})_2]_2$ (**4**) is transformed from a 1-D coordination polymer to a fully 3-D system via Au–Au bonds, and, in $\text{Cu}(\text{tmeda})[\text{Au}(\text{CN})_2]_{1.5}[\text{ClO}_4]_{0.5}$ (**5**), although the dimensionality is unaffected by Au(I), the observed interpenetrating structure is considerably more complex and interconnected as a result of their presence. Thus, aurophilicity can be a powerful design element in generating high-dimensionality, heterometallic systems.

A structural comparison at a deeper level reveals subtle but important details. For example, although **1**, **2**, and $[\text{Cu}(\text{cyclen})\text{Au}(\text{CN})_2][\text{Au}(\text{CN})_2]^{28}$ all contain $\text{Cu}(\text{II})$ centers with four amine donors, they exhibit substantially different structures. An interpretation of this fact requires a consideration of at least three other factors that help to determine the final, observed supramolecular structure: (1) metal coordination geometry, (2) weak hydrogen bonding, and (3) molecular shape.

In **1**, the tetradentate tren ligand caps and sterically crowds one side of the $\text{Cu}(\text{II})$, effectively yielding a five-coordinate $\text{Cu}(\text{II})$ center, while the two bidentate en ligands in **2** can occupy the equatorial plane and allow trans-axial coordination of two additional ligands to occur to the resulting octahedral $\text{Cu}(\text{II})$ center. The ability of en to fashion trans-axial binding sites that are sterically unhindered (while tren cannot) is an important factor that influences the observed structure. The geometry of the ancillary ligands and the subsequent impact on the $\text{Cu}(\text{II})$ coordination geometry thus help determine the final solid-state structure.

There are no aurophilic interactions in **1** despite their important role in **2** and in the related $[\text{Cu}(\text{cyclen})\text{Au}(\text{CN})_2][\text{Au}(\text{CN})_2]$. Both tren and cyclen are tetradentate, capping amine ligands, but one important difference is their hydrogen-bonding capability. Despite the lack of aurophilic interactions in **1**, the ionic units do not form isolated ion pairs, but are connected in an intermolecular fashion by a series of weak to moderate hydrogen bonds to yield a three-dimensional array. Each amine-hydrogen atom forms an intermolecular hydrogen bond to one of the three unbound cyanide nitrogen acceptors, with $\text{N}(\text{amine})-\text{N}(\text{cyanide})$ distances ranging from 3.015(15) to 3.255(17) Å for $\text{N}(1)-\text{N}(22)$ and $\text{N}(10)-\text{N}(22)$, respectively. As aurophilic interactions have the same order-of-magnitude strength (20–50 kJ/mol)^{13,45} as weak hydrogen bonds, these two types of interactions can compete with each other to determine the final structure. The tren ligand has three $-\text{NH}_2$ groups which can hydrogen bond in many directions simultaneously. However, in cyclen there are four $-\text{NH}$ groups; thus fewer hydrogen bonds can be formed, and those that exist have a higher directionality. In $[\text{Cu}(\text{cyclen})\text{Au}(\text{CN})_2][\text{Au}(\text{CN})_2]$ there is indeed one moderate hydrogen-bond interaction between each $-\text{NH}$ group and one unbound N -cyanide atom.²⁸ This hydrogen-bonding network does not disrupt the formation of aurophilic interactions, whereas the multidirectional array of hydrogen bonds that exists in **1** overpowers any attempt to form Au–Au bonds in this system. Weak $\text{Au}-\text{CN}(2)\cdots\text{H}-\text{N}(3)$ interactions ($\text{N}(2)\cdots\text{N}(3) = 3.183(7)$ Å) present in the structure of **2** may play a role in controlling

(61) Jensen, P.; Batten, S. R.; Fallon, G. D.; Hockless, D. C. R.; Moubaraki, B.; Murray, K. S.; Robson, R. *J. Solid State Chem.* **1999**, *145*, 387.

(62) Manson, J. L.; Incarvito, C. D.; Rheingold, A. L.; Miller, J. S. *J. Chem. Soc., Dalton Trans.* **1998**, 3705.

(63) Navarro, R. In *Magnetic Properties of Layered Transition Metal Compounds*; de Jongh, L. J., Ed.; Kluwer Academic Publishers: Dordrecht, 1990; p 105.

(64) White, C. A.; Yap, G. P. A.; Raju, N. P.; Greedan, J. E.; Crutchley, R. J. *Inorg. Chem.* **1999**, *38*, 2548.

(65) (a) Manson, J. L.; Kmety, C. R.; Huang, Q.-Z.; Lynn, J. W.; Bendele, G. M.; Pagola, S.; Stephens, P. W.; Liable-Sands, L. M.; Rheingold, A. L.; Epstein, A. J.; Miller, J. S. *Chem. Mater.* **1998**, *10*, 2552. (b) Manson, J. L.; Arif, A. M.; Miller, J. S. *J. Mater. Chem.* **1999**, *9*, 979. (c) Batten, S. R.; Jensen, P.; Moubaraki, B.; Murray, K. S.; Robson, R. *Chem. Commun.* **1998**, 439. (d) Batten, S. R.; Jensen, P.; Kepert, C. J.; Kurmoo, M.; Moubaraki, B.; Murray, K. S.; Price, D. *J. Chem. Soc., Dalton Trans.* **1999**, 2987. (e) Kurmoo, M.; Kepert, C. J. *New J. Chem.* **1998**, *22*, 1515.

(66) Fukita, N.; Ohba, M.; Okawa, H.; Matsuda, K.; Iwamura, H. *Inorg. Chem.* **1998**, *37*, 842.

the supramolecular arrangement of the ions in **2** as well.³² Note that in **4**, where the methylation of the amine ligands prevents hydrogen-bonding interactions, aurophilic interactions play a dominant role in increasing structural dimensionality from 1 to 3. Thus, reducing hydrogen-bonding interactions could allow for an increased impact of aurophilic interactions on the observed structure, although it is also an excellent strategy to use both Au–Au and hydrogen bonding *in concert* to generate high-dimensionality structures.¹⁴

Finally, the molecular shape of the cationic unit itself may also influence the final structure. For example, the [Cu(en)₂]²⁺ cation may help to template the formation of the extended structure of **2**, as has been reported for {[Cu(en)₂][KCr(CN)₆]}_∞.⁶⁷ Viewed down the *c* axis, the chains of staggered [Au(CN)₂][−] units are cross-linked by stacks of [Cu(en)₂]²⁺ cations which fit well into the space between the dicyanoaurate chains, with a Cu⋯Cu distance of 4.604 Å. An examination of the structures of other CuL₂[Au(CN)₂]₂ complexes (L = 1,2-diaminopropane etc.) would illuminate this point further.

Ag versus Au. Our synthesis and structure of [Cu(en)₂Au(CN)₂][Au(CN)₂] (**2-Au**) allows us to make a comparison with the previously reported dicyanoargentate analogue, [Cu(en)₂Ag(CN)₂][Ag(CN)₂] (**2-Ag**).³² Although **2-Ag** crystallizes in a different space group (*Pnmm*) than **2-Au**, the two systems are practically isostructural. Both are two-dimensional by virtue of cationic [(en)₂Cu–NC–M–CN]⁺ chains cross-linked with roughly orthogonal chains of [M(CN)₂][−] anions (M = Ag, Au), and both structures have a similar weak hydrogen-bonding network. The most important difference between the two lies in the [M(CN)₂][−] units. The Ag(1)–Ag(2) distance in **2-Ag** is 3.1580(5) Å, slightly *longer* than the 3.1405(2) Å in **2-Au**, confirming that aurophilic interactions are stronger than argentophilic interactions. Clean comparisons of metallophilic bond lengths such as this are rare as there are very few M–M bond-containing systems which are identical except for an Ag(I) for Au(I) substitution, as is the case for **2**. As well, the M–C bond lengths in **2-Ag** of 2.050(4) and 2.054(4) Å are significantly

longer than the 1.986(8) and 1.982(7) Å in **2-Au**. This result supports the concept that Au(I) is slightly smaller than Ag(I). Metal-size comparisons based on M–phosphine and M–arsine bond lengths in isostructural compounds,⁶⁸ as well as theoretical calculations,^{13,69} also indicate that Au(I) is smaller than Ag(I).

Conclusions

This work has illustrated that aurophilic interactions can be powerful implements to increase structural dimensionality in supramolecular systems and that Au–Au bonding should be included in the crystal engineering toolbox. Other factors, including the presence of competing/cooperative hydrogen-bonding networks, can also play a role in determining the final solid-state structure. We have also shown that aurophilic interactions can be used as a *tool* to influence the supramolecular structure of systems containing other metals in addition to gold. In principle, aurophilic interactions could be used not only to control the supramolecular arrangement of heterometallic, inorganic polymers but of organic systems as well.

Hence, the introduction of Au(I) centers into molecular systems and the resulting gold–gold interactions are viable design elements in the synthesis of supramolecular complexes in general.

Acknowledgment. Financial support was provided by Simon Fraser University and NSERC of Canada (D.B.L.). Professors R. C. Thompson (University of British Columbia) and N. L. Frank (University of Washington) are gratefully acknowledged for assistance with obtaining SQUID magnetic data.

Supporting Information Available: Complete crystallographic data in CIF format for all four reported crystal structures. This material is available free of charge via the Internet at <http://pubs.acs.org>.

IC010756E

(67) Yuan, A.; Zou, J.; Li, B.; Zha, Z.; Duan, C.; Liu, Y.; Xu, Z.; Keizer, S. *Chem. Commun.* **2000**, 1297.

(68) (a) Bachman, R. E.; Andretta, D. F. *Inorg. Chem.* **1998**, *37*, 5657. (b) Bayler, A.; Schier, A.; Bowmaker, G. A.; Schmidbaur, H. *J. Am. Chem. Soc.* **1996**, *118*, 7006. (c) Tripathi, U. M.; Bauer, A.; Schmidbaur, H. *J. Chem. Soc., Dalton Trans.* **1997**, 2865.
 (69) Bowmaker, G. A.; Schmidbaur, H.; Krüger, S.; Rösch, N. *Inorg. Chem.* **1997**, *36*, 1754.
 (70) Prince, E. *Mathematical Techniques in Crystallography and Materials Science*; Springer-Verlag: New York, 1994.
 (71) Carruthers, J. R.; Watkin, D. J. *Acta Crystallogr.* **1979**, *A35*, 698.